

**Expression of Interest
to Perform a High-Statistics
Neutrino Scattering Experiment
using a Fine-grained Detector
in the NuMI Beam**

November 21, 2002

Argonne National Laboratory - University of Athens - University of
California/Irvine - University of Colorado - Duke University - Fermilab - Hampton
University - Illinois Institute of Technology - James Madison University - Jefferson
Lab - Massachusetts Institute of Technology - University of Minnesota - University of
Pittsburgh - Rutgers - University of South Carolina - Tufts University

Abstract

The NuMI Facility at Fermilab will provide an extremely intense beam of neutrinos for the MINOS neutrino oscillation experiment. The spacious and fully-outfitted MINOS near detector hall will be an ideal place for a high statistics ν and $\bar{\nu}$ -nucleon/nucleus scattering experiment. The experiment described here will provide the neutrino cross-sections and measured nuclear effects required by on-and-off axis neutrino oscillation experiments. In addition, with the high NuMI beam intensity, the experiment will either initially address or significantly improve our knowledge of a wide variety of neutrino physics topics of interest and importance to both the Elementary Particle and Nuclear Physics communities.

J. Arrington, D. H. Potterveld, P. E. Reimer, T. Joffe-Minor
Argonne National Laboratory, Argonne, Illinois

C. Andreopoulos, G. Mavromanolakis, P. Stamoulis, N. Saoulidou, G. Tzanakos, M. Zois
University of Athens, Athens, Greece

D. Casper
University of California, Irvine, California

E. R. Kinney
University of Colorado, Boulder, Colorado

D. Dutta
Duke University, Durham, North Carolina

D. Harris, M. Kostin, J. G. Morfín[†], P. Shanahan
Fermi National Accelerator Laboratory, Batavia, Illinois

M. E. Christy
Hampton University, Hampton, Virginia

N. Solomey
Illinois Institute of Technology, Chicago, Illinois

I. Niculescu
James Madison University, Harrisonburg, Virginia

R. Ent, D. Gaskell, C. E. Keppel*, W. Melnitchouk, S. Wood
Jefferson Lab, Newport News, Virginia

A. Bruell
Massachusetts Institute of Technology, Cambridge, Massachusetts

M. DuVernois
University of Minnesota, Minneapolis, Minnesota

S. Boyd, D. Naples
University of Pittsburgh, Pittsburgh, Pennsylvania

R. Gilman, C. Glasshausser, R. Ransome
Rutgers University, New Brunswick, New Jersey

T. Bergfeld, A. Godley, S. R. Mishra, C. Rosenfeld
University of South Carolina, Columbia, South Carolina

H. Gallagher, W. A. Mann
Tufts University, Medford, Massachusetts

* and Hampton University
† Contact person

Contents

1	Introduction	4
1.1	Significance for Future Experiments	5
2	The Fermilab NuMI Facility	6
2.1	The NuMI Near Experimental Hall	6
2.2	The NuMI Neutrino Beam	6
2.3	Non-neutrino Particle Fluxes in the Near Hall	9
3	Neutrino Scattering Physics	10
3.1	Low-energy ν Cross-sections	11
3.1.1	Neutrino (Quasi) Elastic Scattering Cross-sections and Form Factors	13
3.1.2	Neutrino Resonance Production	13
3.2	The Transition from Resonance Production to Deep Inelastic Scattering: Quark-Hadron Duality	14
3.3	Deep Inelastic Scattering: Extracting Parton Distribution Functions	16
3.3.1	High- x_{Bj} Parton Distribution Functions	18
3.4	Studying Nuclear Effects with Neutrinos	19
3.4.1	Low x: Nuclear Shadowing	20
3.4.2	Mid x: Anti-shadowing and the EMC Effect	21
3.4.3	High x: Multi-quark Cluster Effects	22
3.5	Nuclear Effects and the Determination of $\sin^2 \theta_W$	22
3.6	Strange Particle Production by ν and $\bar{\nu}$	22
3.7	Measuring the Contribution of the Strange Quark to the Spin of the Proton	23
4	A Staged Neutrino Scattering Detector Concept	24
4.1	A Fine-grained Fully-active Neutrino Scattering Detector	25
4.1.1	Particle Identification	27
4.2	LH ₂ and LD ₂ Targets	27
5	An Initial Look at Representative Physics Results with the Detector	28
5.1	Measuring Δs	28
5.2	Measuring Nuclear Effects	29
5.3	Studying the High- x_{Bj} Region	31
5.4	Λ^0 Production in an $\bar{\nu}$ Run	32
6	Conclusions	32

1 Introduction

Although we have been using accelerator-produced neutrino beams for over 30 years in dozens of experiments, there is still a surprisingly large amount we do not know about neutrino interactions, particularly low-energy neutrino-nucleus interactions of interest to both the Elementary Particle (EPP) and Nuclear Physics (NP) communities. This is primarily due to the low intensity of previous neutrino beams, a situation that will change in the near future. The upcoming neutrino oscillation experiments around the world are driving the construction of new, very-intense neutrino beamlines. These new beamlines will allow us to establish a very active research program with a detector, located close to the production target, where event rates will be much higher than at the previous generation of neutrino beam facilities. Furthermore, it is these very same neutrino oscillation experiments, with their low-energy neutrinos and massive nuclear targets, which highlight the need for much improved knowledge of low-energy ν -Nucleus interactions. The current knowledge of ν and $\bar{\nu}$ differential and total cross-sections in the elastic and resonance regions is extremely limited with results displaying large experimental errors. In addition, the distortions introduced by massive nuclear targets on observed ν cross-sections as well as on the observed ν energy distribution has only been glanced at over a very limited kinematic range by early low-statistics bubble chamber experiments.

At Fermilab, the new neutrino facility NuMI (Neutrinos at the Main Injector), designed for the MINOS neutrino oscillation experiment, will be based on the Main Injector (MI) accelerator. Although the neutrino beams from the MI do not have the energy and thus kinematic reach of earlier Tevatron neutrino beams, they do yield several orders of magnitude more events per kg-year of detector than the Tevatron neutrino beam. Thus, one can now perform statistically significant experiments with a much larger range of nuclear targets than the massive iron, marble and other high-A detector materials required in the past. That these facilities are designed to study neutrino oscillations points out a further advantage for future neutrino experiments; an excellent knowledge of the neutrino beam will be required to reduce the beam-associated systematics of the oscillation result. To this end, the MIPP [9] experiment (E907) will run before the start of the MINOS experiment and will measure the exact distribution of π 's and K's emerging from the NuMI target for excellent (\pm few %) knowledge of the absolute ν energy spectrum. This knowledge of the neutrino spectrum will also reduce the beam systematics in the measurement of neutrino scattering phenomena.

Combining these properties of the NuMI beam with a fine-grained neutrino detector will allow much improved measurements of ν cross-sections, a direct measurement of nuclear effects in ν -nucleus interactions (including the NC/CC ratio), a study of the poorly known high- x_{Bj} parton distribution functions and the investigation of other important neutrino scattering topics briefly described in this EOI.

1.1 Significance for Future Experiments

Future experiments designed to measure proton decay [1] or extend our knowledge of the lepton sector through measurement of U_{e3} [2] will necessarily involve large detectors and substantial exposures. These experiments will be searching for rare phenomena with neutrino backgrounds: atmospheric neutrinos in the case of proton decay searches and beam-associated backgrounds in the case of U_{e3} searches. There are several clear examples of specific measurements a high-statistics neutrino scattering experiment could make that may significantly reduce the systematic errors faced by these next generation experiments.

The UNO experiment would have a mass of nearly 0.5Mt and would be able to push limits on proton lifetimes to $10^{34} - 10^{35}$ years. Many SUSY GUT models prefer proton decay into strange channels like $p \rightarrow \nu K^+$ [3]. For these searches atmospheric neutrinos pose a background through CC reactions like $\nu_\mu + n \rightarrow \mu^- K^+ n$ where the final μ is missed, or through associated strange particle production like $\nu + p \rightarrow \nu \Lambda K^+$ [1]. As mentioned in Section 3.6, data on these reactions is scarce, particularly at energies near threshold which are relevant for proton decay studies. In design studies carried out by the UNO proto-collaboration, rates for these reactions are estimated to be in the ballpark of 1 event/Mt-yr. Errors on many of the important background processes approach 100%, for instance in Reference [4] the rate $\nu_l N \rightarrow l^- K^+ N$ in an atmospheric flux is estimated to be 0.6 ± 0.5 events / kiloton-year. The ability to do K/π separation and measure strange production rates in neutrino and anti-neutrino reactions would play an important part in helping these large experiments reach their ultimate sensitivities as exposures extend into the Mt-yr range.

Experiments designed to extend the limits on U_{e3} below the existing Chooz - Palo Verde limits [5, 6] face similar issues. Backgrounds to ν_e appearance come primarily from ν_e in the beam as well as π^0 produced through both charged and neutral current channels. Several studies have been carried out and it is clear that while the relative importance of background from different sources depends on the details of the beam and detector, an underlying problem is a lack of data on single π^0 production reactions and low multiplicity exclusive channels. A recent measurement by the K2K collaboration demonstrates that at an energy of 1.5 GeV, several mechanisms contribute to a single pion sample, including resonant single pion production, coherent pion production, and feed-down from other inelastic channels where nuclear absorption of additional hadrons plays a significant role[7]. As pointed out in [8], it is important to understand not only the rate of background events but the relative contributions from different channels.

In this regard, a dedicated high-statistics experiment could contribute a great deal. With the ability to resolve low energy particles one could make detailed measurements of the various resonant channels. Data taken with different A targets will provide a handle on both the relative amounts of coherent / non-coherent production (the cross section/nucleus is $\propto A^{1/3}$ for coherent processes and $\propto A$ for non-coherent processes) as well as the effects of nuclear scattering and absorption on hadronic final states. The ability to identify μ by their decay also provides the opportunity to fully measure the y-distribution for CC events.

The possibilities for $\nu \bar{\nu}$ running also provide additional handles.

The costs for the next generation of experiments will be significant, typically many tens to hundreds of millions of dollars. The information that could be obtained at a modest cost in a dedicated neutrino scattering experiment could play an important role in helping these experiments achieve their maximum discovery potential.

2 The Fermilab NuMI Facility

The Fermilab NuMI on-site facility is made up of the technical beamline components (target, two magnetic focusing horns, evacuated decay pipe, monitoring devices), the underground facilities to contain and shield these beamline components and a large, on-site experimental detector hall ~ 100 meters underground. The length of the target hall from target to decay pipe is 50 m long. The decay pipe is 675 m long and the hadron absorber hall is 10 m long. Finally, there is a 240 m long dolomite (dirt) muon shield between the hadron absorber and the near detector hall.

2.1 The NuMI Near Experimental Hall

The upstream end of the near detector hall is just over 1 km downstream of the target. This experimental hall is being constructed and completely outfitted for the MINOS near detector. The hall is 45 m long, 9.5 m wide and 9.6m high. As shown in Figure 1, there is a space upstream of the MINOS near detector amounting to, roughly, a cylinder 26 m long and 3m in radius for additional detector(s) which, were it desired, could use the MINOS near detector as an external forward-muon identifier and spectrometer.

2.2 The NuMI Neutrino Beam

The neutrino energy distribution of the NuMI beam can be chosen by changing the distance of the target and second horn with respect to the first horn, as in a zoom lens. There are three standard configurations foreseen for the target and second horn called simply low-energy (le), medium-energy (me) and high-energy (he). The charged-current (CC) event rates for the three tunes are (per 10^{20} protons on target (POT) - ton of detector): le - 80K; me - 270K; he - 630K events. The neutrino energy distributions are shown in Figure 2. It is now expected that the Main Injector will deliver 2.5×10^{20} POT/year at the start of MINOS running, and build up to 3.8×10^{20} POT/year after the first several years of running if the necessary funds can be obtained. The CC event rates per ton (of detector) - year at startup of MINOS in 2005 and the possibly improved rate when a ν scattering experiment could control the beam are summarized in the following table:

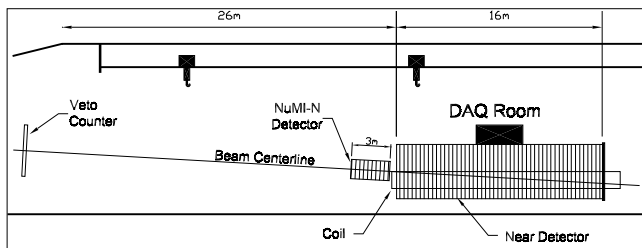


Figure 1: An elevation view of the NuMI near hall emphasizing the large space available for new detector(s). A detector 2 m high by 3 m long, attached to the front of the MINOS near detector, is shown for scale

Event Rates per ton of detector per year		
Beam	Total CC 2005	Eventual Total CC
le	200 K	300 K
me	675 K	1026 K
he	1575 K	2400 K

To be conservative, all event rates in this EOI will assume 2.5×10^{20} POT/year.

The energy of the beamline can also be varied, essentially continuously, by simply varying the distance of target from the first horn and leaving the second horn fixed in the le position. These configurations are called "pseudo"-me/he beams. There is a loss of event rate with this procedure and the most efficient energy tunes always will involve moving the second horn. For the MINOS experiment the beamline will be operating mainly in its lowest possible neutrino energy configuration to be able to reach desired low values of δm^2 . However, to minimize systematics, there will also be running in the pseudo-me and pseudo-he configurations described above. For a possible MINOS running cycle consisting of 12 months le, 3 months pseudo-me and 1 month pseudo-he exposures, with the MI delivering 2.5×10^{20} POT/year, the sum would be order 430 K CC-events/cycle-ton with a neutrino energy distribution shown in Figure 3. For the approved MINOS run consisting of two such cycles (32 months) the total CC event rate would be 860 K/ton. Of this event rate, 140 K/ton would be quasi-elastic, 360 K/ton would be resonance/transition events and 360

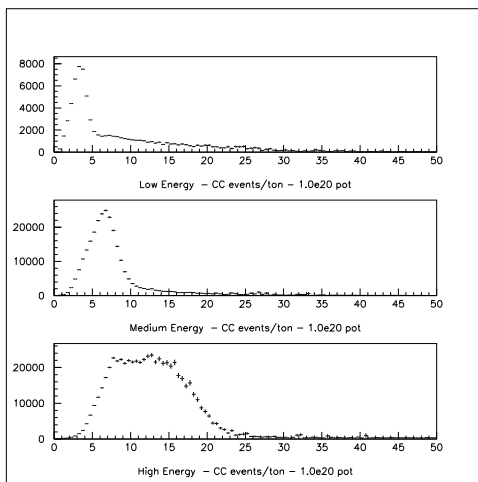


Figure 2: The neutrino event energy distribution for the three configurations of the NuMI beam corresponding to low-energy (le), medium-energy (me) and high-energy (he).

K/ton would be deep-inelastic (DIS) with $W \geq 2 \text{ GeV}$ and $Q^2 \geq 1.0 \text{ GeV}^2$.

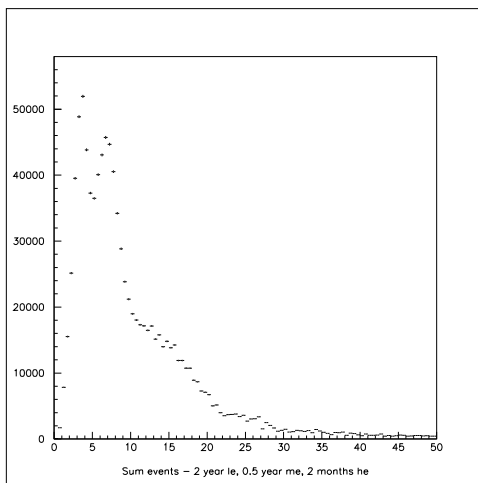


Figure 3: The neutrino event energy distribution for a possible MINOS running cycle as described in the text.

For a NuMI neutrino scattering experiment as prime user of the NuMI beam, the beam-line would be run in the high-energy configuration with energies in the 5 - 25 GeV range. This configuration offers the ability to study neutrino interactions across an appreciable fraction of the x_{Bj} range at reasonable Q^2 . With intensities of 1575 K CC events/ton, which is over a factor 100 higher event rate than NuTeV, experiments could be performed on lighter targets with excellent statistics. A NuMI neutrino scattering experiment, for example, running with the he-beam for a 1 year ν and a 2 years $\bar{\nu}$ period would accumulate

1575 K CC ν events/ton and 900 K CC $\bar{\nu}$ events/ton. Of these 900 K CC ν events/ton and 350 K CC $\bar{\nu}$ events/ton would be DIS. Some of the kinematic distribution of an he- ν run are shown in Figure 4. The total event sample in the top (a) plot is 1575 K events. Of these, 20% have $x_{Bj} \leq 0.10$.

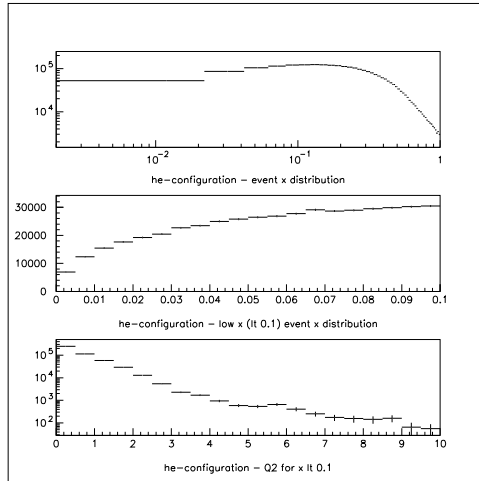


Figure 4: The relative event distributions for an he-configuration run: a) the x_{Bj} distribution for all events; b) the x_{Bj} distribution for events with $x_{Bj} \leq 0.10$; c) the Q^2 distribution for events with $x_{Bj} \leq 0.10$.

The event rates for various scenarios are summarized in the following table giving events/ton-year where a "year" is defined as 2.5×10^{20} POT.

Event Rates per ton of detector			
Run Period	Total CC	Elastic	DIS
MINOS: 3yr	860 K	140 K	360 K
he- ν : 1yr	1575 K	200 K	900 K
he- $\bar{\nu}$: 2yr	900 K	60 K	350 K

2.3 Non-neutrino Particle Fluxes in the Near Hall

Several of the physics topics listed in the next section are sensitive to background interactions caused, particularly, by neutrons. N. Mokhov and M. Kostin [10] from Fermilab have used the MARS Particle Transport Model to perform detailed calculations of these backgrounds. The majority of these background particles come from ν interactions in the rock surrounding the Near Hall. They find the following particle densities directly upstream of the MINOS near detector, for the indicated threshold energy, for the three beam configurations. The units are 10^{-5} per cm^2 per spill. Multiplying these numbers by the

actual fiducial volume of the detector will yield the total integrated path-length, within the volume, of the particle in question.

Particle Flux: units of 10^{-5} per cm^2 per spill				
Particle	E_{th} MeV	le beam	me beam	he beam
n	1	1.745	3.812	8.404
	20	1.088	2.490	4.551
	100	0.472	1.112	1.992
h^\pm	20	0.529	1.105	2.938
	100	0.395	1.078	2.454
γ	20	2.557	4.472	12.570
	100	0.913	1.304	4.208
e^\pm	20	1.246	2.144	4.921
	100	0.403	0.703	2.209
μ^\pm	20	3.450	6.690	11.580
	100	3.448	6.560	11.320

The geometry of the situation, and consequently the rates, change with the side muon-identifiers in place. Under the reasonable assumption that we will be able to see ν interactions in the side counters and exclude potential backgrounds in the fiducial volume of the central detector that are kinematically consistent with them, the side counters cut the neutron background ($E \geq 50$ MeV) by a further 50 %, the charged hadron background by 25 % and the muon background by 10 %. On the other hand, the presence of the side counters increase the background of γ 's and electrons by 15 % and 7 % respectively. As an example, since neutron background seems to offer the biggest challenge to some physics topics to be discussed, in the fiducial volume ($r = 80$ cm, $l = 150$ cm) of the detector to be described in Section 4, there is a total track length of 6.5 cm for neutrons with $E_{th} \geq 100$ MeV or $\approx 0.08 \lambda_I$ when using the le-beam. On top of this, the energy transfer to the final state must be included before estimating the background for any physics search. These background fluxes have been estimated without taking any measures to lower the backgrounds even further should the physics require it. Since the neutrons are not thermal, there are effective methods for reducing the flux. For comparison, the probability for a ν interaction in the fiducial volume per spill is $\approx 0.1/\text{spill}$ during the MINOS exposure and $\approx 0.18/\text{spill}$ during an he- ν run.

3 Neutrino Scattering Physics

A neutrino scattering experiment in the NuMI Near Experimental Hall will offer a unique opportunity to study a diverse array of physics topics. Most of these topics have either never

been studied or the few results that do exist are plagued by large statistical and systematic errors. In addition to being significant fields of study in their own right, many of these topics are essential to help minimize the systematics of neutrino oscillation experiments. Among the topics that can be studied:

- quasi-elastic neutrino scattering
- the poorly studied resonance production region
- the intriguing region where resonance production joins deeply inelastic scattering
- parton distribution functions (pdf), particularly in the high- x_{Bj} region
- leading exponential contributions of pQCD
- $\sin^2 \theta_W$ via the ratio of NC / CC as well as $d\sigma/dy$ from ν - electron scattering to check the recent surprising NuTeV result
- charm physics including the mass of the charm quark (m_c) to an order of magnitude better accuracy than current values, V_{cd} , $s(x)$ and, independently, $\bar{s}(x)$
- nuclear effects involving neutrinos. In particular are nuclear effects the same for charged lepton and ν interactions and for different quarks flavors? Can nuclear effects explain the NuTeV result mentioned above?
- strange particle production for V_{us} , flavor-changing neutral currents and measurements of hyperon polarization
- contribution of the strange quark to the spin of the proton through ν elastic scattering. This measurement is far more accurate and needs many fewer assumptions than charged lepton results for Δs .
- nuclear physics studies with neutrinos, complementary to JLab studies in the same kinematic range, but with the weak force, the addition of the axial-vector current and the ν 's ability to isolate specific quark flavors.

3.1 Low-energy ν Cross-sections

This is a topic of considerable importance for neutrino oscillation experiments, which are forced to use very low energy neutrino beams to reach the pertinent values of δm^2 . The cross-sections in this kinematic regime are not only the comparatively well-measured deep-inelastic cross-section but also include the elastic and resonance cross-sections. The available measurements from early experiments at ANL, BNL, CERN and FNAL all have considerable errors due to low statistics and lack of knowledge of the incoming flux [11]. In addition, even with these large errors, the results are often conflicting. A standing working

group [14] has been established to assemble all available data on ν and $\bar{\nu}$ cross-sections and to determine quantitative requirements for new experiments. A summary of the total ν and $\bar{\nu}$ cross-sections are shown in Figure 5 [12] and Figure 6 respectively.

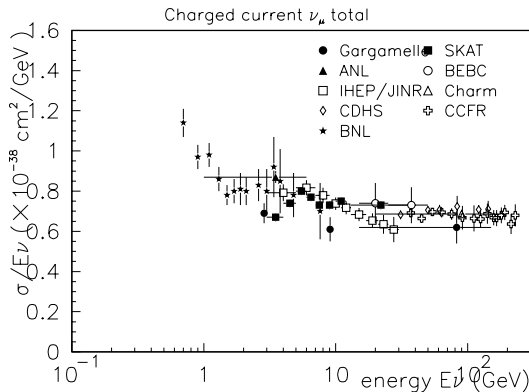


Figure 5: The current status of the total ν cross-section measurements

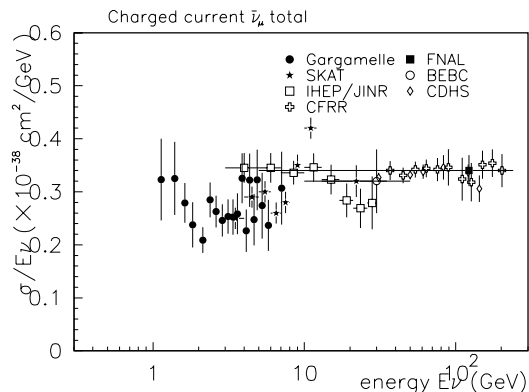


Figure 6: The current status of the total $\bar{\nu}$ cross-section measurements

Another, totally independent effect, which must be considered for $d\sigma/dQ^2$ at low Q^2 , is PCAC. As $Q^2 \rightarrow 0$ the vector current is conserved and goes to zero but the axial-vector part of the weak current is only partially conserved (PCAC) and $F_2(x, Q^2)$ approaches a non-zero constant value as $Q^2 \rightarrow 0$. According to the Adler theorem [35], the cross section of $\nu_\mu - N$ can be related to the cross section for $\pi - N$ at $Q^2 = 0$. CCFR has made initial measurements [36] of this effect with neutrinos off an Fe target with no attempt to correct for possible neutrino specific nuclear effects which will be discussed shortly.

The important topic of nuclear distortions of neutrino-induced final states will be discussed in detail shortly. It is, however, worth noting here that the lack of knowledge of low-energy ν cross-sections is only compounded by the effects of nuclear targets. In modeling expectations for visible final states and energy distributions one must include

the effects of Pauli suppression, Fermi motion, nucleon-nucleon correlations, nuclear transparency and general final-state interactions. The inclusion of Pauli suppression effects is relatively straight-forward, however the treatment of Fermi motion effects is not yet clear. The use of the Bodek-Ritchie [37] model for Fermi motion has been shown to be acceptable at low Fermi momentum but becomes increasingly inaccurate at higher Fermi momentum [38]. An attempt to remedy this situation is being undertaken by the MINOS collaboration using nuclear spectral functions [39]. Accurate measurements off different nuclei provided by this experiment can help determine the correct formulation of the high Fermi momentum tail.

3.1.1 Neutrino (Quasi) Elastic Scattering Cross-sections and Form Factors

The physics of (quasi) elastic neutrino scattering was summarized in an early publication of Lewellyn-Smith [40]. He expresses the scattering in terms of weak and electromagnetic form factors. Some of the measurements of these form factors can be taken from e/μ -nucleon scattering while others need ν -nucleon scattering. The current status of measurements of the ν and $\bar{\nu}$ elastic cross-sections are shown in Figure 7 and Figure 8. As can be seen, there is considerable spread for the values of σ_{el} for any given ν energy.

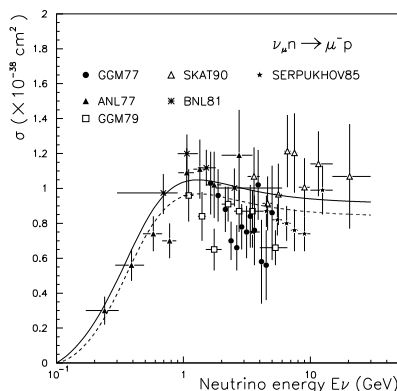


Figure 7: The current status of ν quasi-elastic cross-section measurements. The curves are the Lewellyn-Smith prediction with and without Pauli suppression.

3.1.2 Neutrino Resonance Production

There is very little data on neutrino resonance production. Neutrino monte carlo programs trying to cover this kinematic region have been using early theoretical predictions by Rein and Sehgal [15] or results from electro-production experiments. Recently Paschos [16] has contributed to this study concentrating on how charge exchange of one-pion final states enters into neutrino oscillation analyses. Lee and Sato [13] have expanded their work on the electroproduction of resonances to include neutrino production of the Δ resonance as well. The experimental results for the one- π states are summarized in Figure 9.

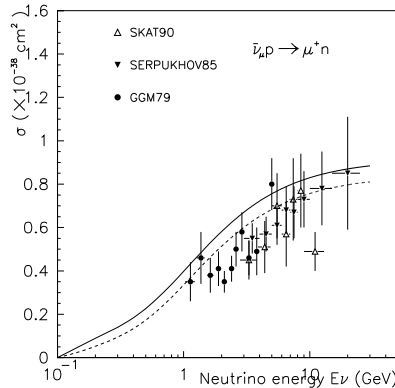


Figure 8: The current status of $\bar{\nu}$ quasi-elastic cross-section measurements. The curves are as in the preceding figure.

3.2 The Transition from Resonance Production to Deep Inelastic Scattering: Quark-Hadron Duality

At high energies an efficient description of scattering phenomena is afforded in terms of quarks. However, at low energies, where the effects of confinement make strongly-coupled QCD highly non-perturbative, it is more efficient to work in terms of collective degrees of freedom, the physical mesons and baryons. We know that in principle it should just be a matter of convenience in choosing to describe a process in terms of quark-gluon or hadronic degrees of freedom. This principle is referred to as *quark-hadron duality*, and means that one can use either set of complete basis states to describe physical phenomena. The duality between quark and hadron descriptions reflects the relationship between confinement and asymptotic freedom and is intimately related to the nature of the transition from non-perturbative to perturbative QCD.

Although the duality between quark and hadron descriptions is formally exact in principle, how this reveals itself specifically in different physical processes and under different kinematical conditions is the key to understanding the consequences of QCD for hadronic structure. The phenomenon of duality is in fact quite general in nature and can be studied in a variety of processes, such as $e^+e^- \rightarrow$ hadrons, or semi-leptonic decays of heavy quarks. In lepton-nucleon scattering, duality links the physics of resonance production to the physics of scaling, historically called Bloom-Gilman duality[18].

Recent Bloom-Gilman duality results from Jefferson Lab [17, 19, 20, 21, 22] for the proton F_2 , R , F_1 , F_L , and g_1 structure functions, as well as F_2 in nuclei (even the EMC effect is reproduced by the resonance region), agree very well on average with available deep inelastic parameterizations. It is a surprise that the deep inelastic, “single-quark”, curves describe both the average resonance strength and Q^2 dependence so well, to better than 10%, to Q^2 values as low as ≈ 1 (GeV/c) 2 . Though not yet well understood theoretically, it appears that duality is a fundamental aspect of nucleon structure and may provide crucial information in understanding the transition from non-perturbative to perturbative QCD.

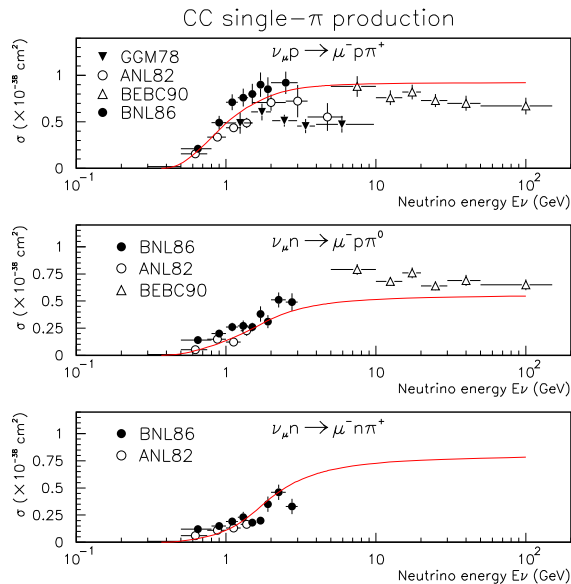


Figure 9: Existing measurements of neutrino-induced 1-pion production. The curve is the Rein-Sehgal model prediction.

Testing duality in neutrino structure functions will be an exciting avenue in developing an understanding of this phenomena. There could, in fact, be qualitative differences between the workings of duality in electron and neutrino structure functions. Measurements from this proposed experiment will allow similar analyses to be performed with resonance production from ν interactions which, with contributions of the axial-vector current, will be different from any previous duality studies.

At very low Q^2 , (≤ 0.8 (GeV/c) 2), duality appears to break down, and it has been observed that the average resonance behavior (i.e. duality data) take a valence-like shape [23] in electron-scattering more quickly than lower x data. There is at least one approved experiment to test this observation further in electron scattering, and neutrino scattering is an obvious regime for investigating this valence behavior as well.

It is important to point out also a revolutionary application of duality: if the workings of the resonance—deep-inelastic interplay are understood, the region of very high x will become more accessible. The region of $x \approx 1$ is an important testing ground for mechanisms of spin-flavor symmetry breaking in valence quark distributions. In addition, with nuclear targets it would permit measurement of the nuclear medium modification of the nucleon structure function at large x , where the deviation from unity of the ratio of nuclear to nucleon structure functions is largest, and sensitivity to different nuclear structure models greatest.

How to incorporate quark-hadron duality into neutrino Monte Carlos is being discussed. A recent analysis by Bodek and Yang[27] seems to offer a very promising procedure for fitting structure functions in the low Q^2 , high x region. Extrapolating their results through

the resonance region yields values of F_2 consistent with duality results from Jefferson Lab.

3.3 Deep Inelastic Scattering: Extracting Parton Distribution Functions

One of the obvious reasons for the significance of neutrino results in the extraction of parton distribution functions is the neutrino's ability to directly resolve the flavor of the nucleons constituents: ν interacts with d, s, \bar{u} and \bar{c} while the $\bar{\nu}$ interacts with u, c, \bar{d} and \bar{s} . This unique ability of the neutrino to "taste" only particular flavors of quarks enhances any study of parton distribution functions. This high-statistics study of the partonic structure of the nucleon, using the neutrino's weak probe, would complement the on-going study of this subject with electromagnetic probes at Jlab.

The QCD evolution of parton distribution functions takes high- x_{Bj} pdf's at low Q and evolves them down to moderate-and-low- x_{Bj} at higher Q. This obviously means that one of the larger contributions to background uncertainties at LHC measurements will be the very poorly known high-x pdf's at the lower Q values open to NuMI neutrino beams. That there appears to be an unexplained anomaly at high- x_{Bj} will be discussed shortly. The problem in studying this point has been the accumulation of sufficient statistics at high- x_{Bj} , off of light targets, to extract the pdf's. The NuMI beam will yield the necessary statistics to start addressing this major concern.

With the high statistics foreseen at NuMI as well as the special attention to minimizing neutrino beam systematics, it should be possible for the first time to eventually determine the separate structure functions $F_1^{\nu N}(x, Q^2)$, $F_1^{\bar{\nu} N}(x, Q^2)$, $F_2^{\nu N}(x, Q^2)$, $F_2^{\bar{\nu} N}(x, Q^2)$, $x F_3^{\nu N}(x, Q^2)$ and $x F_3^{\bar{\nu} N}(x, Q^2)$ where N is an isoscalar target.

As an example, in leading order QCD (used for illustrative purposes) four of the structure functions are related to the parton distribution functions by:

$$\begin{aligned}
 2F_1^{\nu N}(x, Q^2) &= u(x) + d(x) + s(x) + \bar{u}(x) + \\
 &\quad \bar{d}(x) + \bar{c}(x) \\
 2F_1^{\bar{\nu} N}(x, Q^2) &= u(x) + d(x) + c(x) + \bar{u}(x) + \\
 &\quad \bar{d}(x) + \bar{s}(x) \\
 xF_3^{\nu N}(x, Q^2) &= u(x) + d(x) + s(x) - \bar{u}(x) - \\
 &\quad \bar{d}(x) - \bar{c}(x) \\
 xF_3^{\bar{\nu} N}(x, Q^2) &= u(x) + d(x) + c(x) - \bar{u}(x) - \\
 &\quad \bar{d}(x) - \bar{s}(x)
 \end{aligned}$$

Note that taking differences and sums of these structure functions would then allow extraction of individual parton distribution functions in a given x, Q^2 bin:

$$\begin{aligned}
2F_1^{\nu N} - 2F_1^{\bar{\nu} N} &= [s(x) - \bar{s}(x)] + [\bar{c}(x) - c(x)] \\
2F_1^{\nu N} - xF_3^{\nu N} &= 2[\bar{u}(x) + \bar{d}(x) + \bar{c}(x)] \\
2F_1^{\bar{\nu} N} - xF_3^{\bar{\nu} N} &= 2[\bar{u}(x) + \bar{d}(x) + \bar{s}(x)] \\
xF_3^{\nu N} - xF_3^{\bar{\nu} N} &= [\bar{s}(x) + s(x)] - [\bar{c}(x) + c(x)]
\end{aligned}$$

As we increase the order of QCD and allow gluons into consideration we need to bring in global fitting techniques into the extraction of the parton distribution functions. However, with the manageable systematic errors expected with the NuMI beam, the ability to isolate individual parton distribution functions will be dramatically increased by measuring the full set of separate ν and $\bar{\nu}$ structure functions with the statistics possible in this experiment.

There are two primary (associated) methods for extracting this full set of structure functions. One can either use the varying y behavior of the coefficients of the structure functions in the expression for the cross section:

$$\begin{aligned}
\frac{d^2\sigma^{\nu(\bar{\nu})}}{dxdy} &= 2\frac{G_F^2 M_p E_\nu}{\pi} \left[xy^2 F_1^{\nu(\bar{\nu})}(x, Q^2) + \right. \\
&\quad \left. \left(1 - y - \frac{M_p xy}{2E_\nu}\right) F_2^{\nu(\bar{\nu})}(x, Q^2) \pm \right. \\
&\quad \left. y(1 - y/2) xF_3^{\nu(\bar{\nu})}(x, Q^2) \right],
\end{aligned}$$

or one can use the "helicity representation" of the cross section:

$$\begin{aligned}
\frac{d^2\sigma^\nu}{dxdQ^2} &= \frac{G_F^2}{2\pi x} \left[\frac{1}{2} (F_2^\nu(x, Q^2) + xF_3^\nu(x, Q^2)) + \right. \\
&\quad \left. \frac{(1-y)^2}{2} (F_2^\nu(x, Q^2) - xF_3^\nu(x, Q^2)) - \right. \\
&\quad \left. 2y^2 F_L^\nu(x, Q^2) \right],
\end{aligned}$$

and

$$\begin{aligned}
\frac{d^2\sigma^{\bar{\nu}}}{dxdQ^2} &= \frac{G_F^2}{2\pi x} \left[\frac{1}{2} (F_2^{\bar{\nu}}(x, Q^2) - xF_3^{\bar{\nu}}(x, Q^2)) + \right. \\
&\quad \left. \frac{(1-y)^2}{2} (F_2^{\bar{\nu}}(x, Q^2) + xF_3^{\bar{\nu}}(x, Q^2)) - \right. \\
&\quad \left. 2y^2 F_L^{\bar{\nu}}(x, Q^2) \right],
\end{aligned}$$

Then, by plotting events as a function of $(1 - y)^2$ in a given $x - Q^2$ bin, it is possible to extract all six structure functions.

3.3.1 High- x_{Bj} Parton Distribution Functions

If we concentrate on the region of high- x_{Bj} , the uncertainties in current nucleon parton distribution functions are of two types: the ratio of the light quark pdf's, $d(x)/u(x)$, as $x \rightarrow 1$ and the role of leading power corrections (higher twist) in the extraction of the high x behavior of the quarks.

Analyses of present leptonproduction data sets that used hydrogen and deuterium targets have been unable to pin down the high- x behavior of $d(x)/u(x)$. An analysis by Bodek and Yang [67] indicated that the $d(x)/u(x)$ quark ratio approaches 0.2 as $x \rightarrow 1$. However global QCD analyses of experimental results, such as the CTEQ fits [72], do not indicate the need for this higher value of $d(x = 1)/u(x = 1)$. Besides the statistical and experimental uncertainties in the existing data sets, a complication with past experimental results was the need to model nuclear binding effects in the deuterium target which was used. These issues could be avoided with a high statistics exposure to a H_2 target which could directly measure the $d(x)/u(x)$ ratio in protons as $x \rightarrow 1$ from the ratio of neutrino-proton to antineutrino-proton cross-sections. Such a measurement would require only a small correction for the residual sea quark contributions at high x .

The measurement of quark densities at high- x_{Bj} is closely related to the question of the leading power corrections known as "higher twist effects". The n^{th} order higher twist effects are proportional to $1/Q^{2n}$ and reflect the fact that quarks have transverse momentum within the nucleon and that the probe becomes larger as Q^2 decreases, thus increasing the probability of multi-quark participation in an interaction. As was the case with the d/u ratio, different analyses of higher twist corrections in current data leave some unresolved issues that would benefit from new experimental information. Recent work by Yang and Bodek [51] seems to indicate that what has been measured as "higher-twist" in charged lepton scattering analysis is essentially accounted for by increasing the order (NNLO) of the perturbative QCD expansion used in the analysis.

The only actual measurements of a higher-twist term in neutrino experiments have been two low-statistics bubble chamber experiments: in Gargamelle [73] with freon and in BEBC [68] with NeH_2 . Both bubble chamber analyses are complicated by nuclear corrections at high- x . However, both analyses found a twist-4 contribution that is smaller in magnitude than the charged leptonproduction analysis and, most significantly, is preferentially negative.

There are several indications that current parameterizations of the pdf's are **not** correct at high- x_{Bj} . Figure 10 shows the ratio of measured Drell-Yan pair production [52] compared to the latest CTEQ global fits, CTEQ6 [53]. The comparison seems to indicate that the valence distributions are **OVERestimated** at high- x_{Bj} . This is in direct contrast to a recent analysis at Jefferson Lab which seems to indicate that the valence distributions are **UNDERestimated** at high- x_{Bj} as in Figure 11.

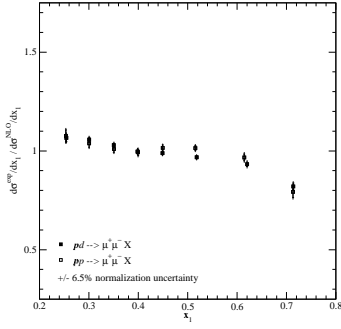


Figure 10: Ratio of data to predictions based on CTEQ6 NLO pdf's vs x_1

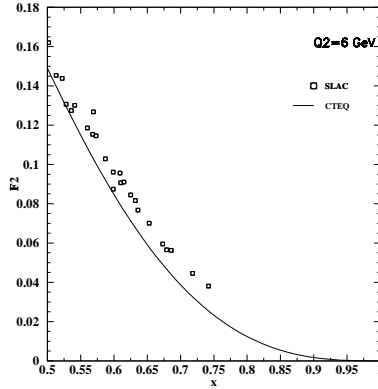


Figure 11: Results from SLAC electron scattering experiments compared to the CTEQ6 NLO prediction at high- x_{Bj}

Efforts are underway to understand how the $d(x)/u(x)$ ratio enters into this particular experimental comparison. The large sample of high- x_{Bj} events in this experiment would certainly help understand these results.

3.4 Studying Nuclear Effects with Neutrinos

Nuclear effects in DIS measurements of structure functions have been studied extensively using muon and electron beams yielding the phenomena sketched in Figure 12 for the ratio of F_2 from a heavy nuclear target to F_2 from a deuterium target.

These nuclear effects have only been glanced at for neutrinos in low-statistics bubble chamber experiments. Furthermore, there is hardly any data on nuclear effects of specific hadronic final states (the fragmentation functions) for any incoming lepton. These effects

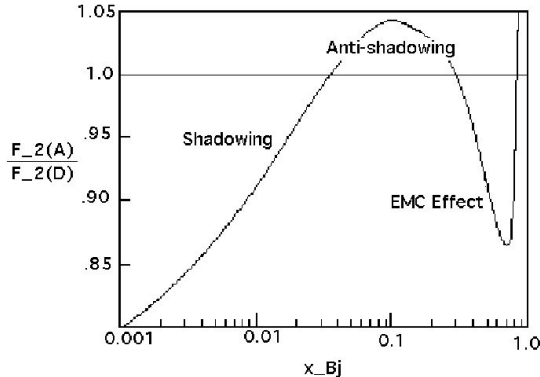


Figure 12: The general observed behavior of the ratio of measured F_2 with of a heavy nuclear target to F_2 with deuterium as a function of x_{Bj}

are expected to be large [16] and particularly important for neutrino energies producing a data sample with a large fraction of elastic and resonant final states.

High statistics neutrino experiments have, to date, only been possible using heavy nuclear targets such as iron-dominated target-calorimeters and, for these targets, nuclear effects in $\nu - N$ interactions have typically been considered as problems to overcome rather than as a source of physics insights. A neutrino scattering program at NuMI would provide experimental conditions where a systematic, precision study of both fragmentation and structure functions would be possible by using a variety of heavy nuclear targets as well as H_2 and D_2 targets. Briefly reviewing the nuclear effects on measured structure functions as a function of x_{Bj} we find [28]:

3.4.1 Low x : Nuclear Shadowing

In the shadowing region, $x < 0.1$, there are several effects where a neutrino probe could provide different insights compared to charged lepton probes. "Shadowing" is a phenomena which occurs with nuclear targets and is characterized by the cross section per nucleon being less for larger A nuclei, such as Fe, than for smaller A nuclei such as D_2 . See [34] for a recent summary of theoretical thinking on this topic.

Vector meson dominance (VMD) is the accepted explanation for shadowing in the scattering of charged leptons off nuclei (i.e. $\mu/e - A$) for Q^2 roughly $\leq 5 \text{ GeV}^2$. In essence, the incoming boson dissociates into a $q-\bar{q}$ pair which interacts with the nucleus as a meson. Due to the V-A nature of the weak interaction, it is predicted that neutrino scattering should involve not only a VMD effect but also additional contributions from axial-vector mesons such as the A_1 . Other sources of nuclear shadowing (mainly in larger nuclei) involve gluon recombination from nucleons neighboring the struck nucleon that shift the parton distri-

butions towards higher values of x . At higher Q^2 , shadowing is dominated by Pomeron exchange in diffractive scattering.

A quantitative analysis of neutrino shadowing effects by Kulagin [41] uses a non-perturbative parton model to predict shadowing effects in $\nu - A$ scattering. As seen in Figure 13, which gives predictions of the ratio of scattering off Fe to scattering off D_2 , shadowing effects with neutrinos are expected to be dramatically large at low Q^2 (the kinematic region of the NuMI neutrino beam) and still significant at large Q^2 . Kulagin also attempts to determine the quark flavor dependence of shadowing effects by separately predicting the shadowing observed in $F_2(x, Q^2)$ (sum of all quarks) and $xF_3(x, Q^2)$ (valance quarks only). These predictions of Kulagin should be testable with the NuMI beam.

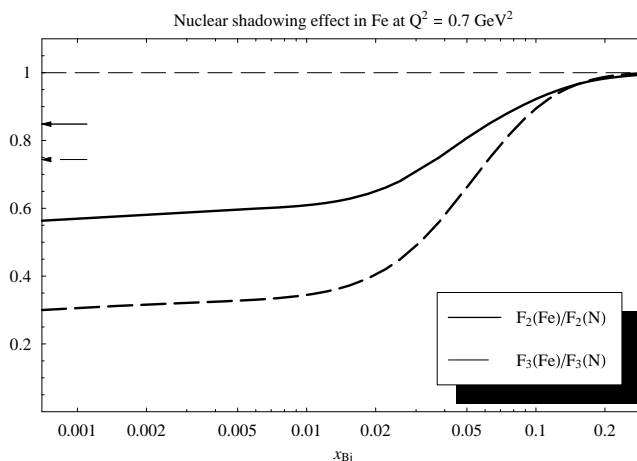


Figure 13: Expected shadowing effects off an Fe target at $Q^2 = 0.7 \text{ GeV}^2$ with Kulagin’s non-perturbative parton model emphasizing the difference in shadowing for F_2 and xF_3 . The arrows in the vicinity of $R = 0.8$ indicate the expected shadowing strength at $Q^2 = 15.0 \text{ GeV}^2$

3.4.2 Mid x: Anti-shadowing and the EMC Effect

Drell-Yan experiments have also measured nuclear effects and their results are quite similar to DIS experiments in the shadowing region. However, in the anti-shadowing region where R_A , the ratio of scattering off a nucleus A to scattering off of deuterium, makes a statistically significant excursion above 1.0 in DIS, Drell-Yan experiments see no effect. This could be an indication of difference in nuclear effects between valence and sea quarks as also predicted by Kulagin.

Eskola et al. [42] has quantified this difference using a model which predicts that the differences between nuclear effects in $xF_3(x, Q^2)$ and $F_2(x, Q^2)$, quantified by Kulagin in the shadowing region, should persist through the anti-shadowing region as well. More recent work by Kumano [43] supports these findings using different fitting techniques.

Based on the various theoretical explanations for the anti-shadowing and EMC effects existing today, the measured effects could be considerably different for neutrinos. Neutrino scattering results would help the theoretical understanding of these phenomena.

3.4.3 High x : Multi-quark Cluster Effects

Analyses from DIS experiments of $F_2(x, Q^2)$ in the "Fermi-motion" region, $x \geq 0.7$, have used few-nucleon-correlation models and multi-quark cluster models in order to fit the data. These models boost the momentum of some quarks, which translates into a high- x tail in $F_2(x, Q^2)$ that is predicted to behave as e^{-ax} . However, fits to $\mu - C$ [44] and $\nu - Fe$ [45] have obtained two different values for the fitted constant a : $a = 16.5 \pm 0.5$ and $a = 8.3 \pm 0.7 \pm 0.7$ (systematic), respectively. This is considered surprising because of the expectation that any few-nucleon-correlation or multi-quark effects would have already saturated by carbon. A high statistics data sample, off several nuclear targets, could go a long way towards resolving the dependence of the value of a on the nucleus and on the lepton probe.

3.5 Nuclear Effects and the Determination of $\sin^2 \theta_W$

There have been many attempts to explain the recent NuTeV [29] measurement of $\sin^2 \theta_W$ which is 3σ away from the Standard Model expectation. Among the most persuasive are the unknown nuclear effect corrections involving neutrinos [30]. This experiment will be able to directly measure the ratio NC / CC on various nuclear targets to determine the nuclear effects experimentally.

3.6 Strange Particle Production by ν and $\bar{\nu}$

As pointed out by Solomey [46] the measurement of both charged and neutral current strange particle production cross-sections would yield new information [31, 32, 33] on the six form factors as well as a very clean measurement of V_{us} . In addition the search for strangeness-changing neutral currents (SCNC) is important as an indication of new physics.

A study of these topics has been difficult since strangeness production by ν is suppressed by a factor of $\tan^2 \theta_c$ (the Cabibbo mixing angle). To date only a handful of experiments have measured a few of these reactions, all with bubble chambers where the particle interaction and secondary particles produced could be explicitly identified. The best results and only cross sections measured is from the CERN-PS Gargamelle bubble chamber experiment [47] with 15 events of Λ^0 CC production at 2×10^{-40} cm²/nucleon; while 7 events exist from the ZGS bubble chamber which includes one neutral current strange particle production event [48].

This experiment, with its extremely high statistics, would enable a search for the charged current (CC) and neutral current (NC) interactions:

$$\bar{\nu}_l + p^+ \rightarrow l^+ + \Lambda^0 \qquad \bar{\nu} + p^+ \rightarrow \bar{\nu} + \Sigma^+ \qquad SCNC$$

$$\begin{array}{lll}
\rightarrow l^+ + \Sigma^0 & \rightarrow \bar{\nu} + \pi^0 + \Sigma^+ & SCNC \\
\rightarrow l^+ + \pi^0 + \Lambda^0 & \rightarrow \bar{\nu} + K^0 + \Sigma^+ & \\
\rightarrow l^+ + \pi^0 + \Sigma^0 & \rightarrow \bar{\nu} + K^0 + p^+ & SCNC \\
\rightarrow l^+ + K^- + p^+ & \rightarrow \bar{\nu} + K^+ + n^0 & SCNC \\
\vdots & \vdots & \\
\bar{\nu}_l + n^0 \rightarrow l^+ + \Sigma^- & \bar{\nu} + n^0 \rightarrow \bar{\nu} + \Lambda^0 & SCNC \\
\rightarrow l^+ + \pi^- + \Lambda^0 & \rightarrow \bar{\nu} + \Sigma^0 & SCNC \\
\rightarrow l^+ + \pi^0 + \Sigma^- & \rightarrow \bar{\nu} + K^0 + \Lambda^0 & \\
\rightarrow l^+ + K^- + \Lambda^0 & \rightarrow \bar{\nu} + K^0 + \Sigma^0 & \\
\vdots & \vdots &
\end{array}$$

3.7 Measuring the Contribution of the Strange Quark to the Spin of the Proton

The role of the strange quark sea in the proton is a central question in both nuclear and particle physics. The most interesting questions are whether the strange quarks contribute substantially to either the quark structure of the proton or to the spin of the proton. With respect to the quark structure, results from parity violating electron scattering, thus far, indicate that the contribution is small[54, 55]. However, recent results from a higher energy neutrino scattering experiment[56], NUTEV, indicate that a substantial fraction of the sea's momentum in the proton is carried by the strange quarks. As far as the spin contribution, it is generally believed that the strange quarks make a negative contribution to the spin of the proton[58, 62, 63, 64, 65, 66]. For example, a recent analysis[57] indicates that $\Delta s = -0.12 \pm 0.03$.

A NuMI ν scattering experiment would be able to significantly address both of these issues [49, 50]. In particular, neutrino elastic scattering from the proton offers a new opportunity to provide a definitive measurement of Δs . The neutrino elastic scattering method is free from the usual assumptions, such as $SU(3)_f$ symmetry, $x \rightarrow 0$ extrapolations and the purity method, used in semi-inclusive deep inelastic scattering at SMC, HERMES or COMPASS.

As discussed by Garvey *et al*[60], neutral current scattering from the proton is very sensitive to the spin carried by the strange quarks in the proton. The coupling of the nucleon's current to the Z^0 is given by

$$\begin{aligned}
j_\mu^N Z^\mu &= \left(\frac{G_F}{\sqrt{2}} \right)^{\frac{1}{2}} \langle N' | F_1^Z(Q^2) \gamma_\mu + \\
&F_2^Z(Q^2) \frac{i\sigma_{\mu\nu} q^\nu}{2M_p} +
\end{aligned}$$

$$G_1^Z(Q^2)\gamma_\mu\gamma^5|N\rangle\cdot Z^\mu$$

where

$$\begin{aligned} F_j^Z(Q^2) \equiv & \left(\frac{1}{2} - \sin^2(\theta_W)\right) [F_j^p(Q^2) - \\ & F_j^n(Q^2)]\tau_3 - \sin^2(\theta_W)[F_j^p(Q^2) + \\ & F_j^n(Q^2)] - \frac{1}{2}F_j^s(Q^2) \end{aligned}$$

and

$$G_1^z(Q^2) \equiv \frac{-G_A(Q^2)}{2}\tau_3 + \frac{G_s(Q^2)}{2}$$

where the notation is that of ref[60]. The $F_j^{p(n)}(Q^2)$ are the proton (neutron) electromagnetic form factors, and $F_j^s(Q^2)$ is the strange contribution to the neutral weak current vector form factor. $G_A(Q^2)$ is the nucleon axial vector form factor and $G_s(Q^2)$ is the strange axial vector form factor. Here, $G_1^s(Q^2 = 0) = \Delta s$. Since the axial strange form factor and the axial vector form factor enter the expression at the same level, it is necessary to either know the nucleon axial form factor very well as in experiment 734 at BNL[59] or to perform the experiment at low Q^2 so that the uncertainty in the axial form factor is minimized[61].

Because of technical considerations, the most practical target/detector device for neutrino elastic scattering is plastic scintillator. (A description of such a detector will be given in the next section on). This means that most of the neutrino scattering is quasi-elastic scattering from the nucleons in the carbon in the scintillator. Thus, nuclear effects must be taken into account. Fortunately, using the **ratio** of neutral current to charge current yields, at a relatively low Q^2 , minimizes the effect of the uncertainty in the axial form factor as well as nuclear corrections.

4 A Staged Neutrino Scattering Detector Concept

In order to perform the full spectrum of physics outlined in this paper, the target/detector must be able to:

- identify muons and measure their momentum with high precision
- measure the energy of both the hadronic and electromagnetic shower with reasonable precision
- identify and measure the energy of protons
- incorporate particle identification (TOF and particle stop/decay) for complete reconstruction of final states
- accommodate other nuclear targets.

4.1 A Fine-grained Fully-active Neutrino Scattering Detector

These goals can be readily met in a staged approach to detector development and installation. For initial running in a parasitic mode with the MINOS experiment and for a he ν exposure, the physics goals can be met by a comparatively simple active target/detector [69] consisting essentially of solid scintillator strips interspersed with occasional planes of variable A target. The detector would have the approximate overall dimensions of a cube 2.0m on a side. Significant granularity would be achieved by the use of 2.0 m long by 2 cm x 2 cm strips of plastic scintillator(CH) with a fiber down the center of the strip for readout. Recent work at the Fermilab Scintillator/VLPC (Visible Light Photon Counter) R&D Facility has shown that using light division across triangularly shaped scintillator strips of this size can yield position precisions of a few mm. The orientation of the scintillator strips is alternated so that 2-dimensional tracking can be performed. The detector overall mass would be around 8 metric tons with somewhat over 3 tons of scintillator in a fiducial volume defined as $r \leq 0.8\text{m}$ and 150 cm long.

The downstream end of this detector would be placed as close as possible to the upstream face of the MINOS near detector in order to use the magnetic field and steel of the MINOS near detector as a muon identifier and spectrometer for the energetic forward going muons as shown in Figure 14. Side muon ID/spectrometers (EMI) consisting of several planes of scintillator interspersed with (permanent magnet?) steel planes would be installed surrounding the four sides of the detector to increase acceptance of the low energy muons and measure the hadronic energy leaving the sides of the central detector. Figure 15 shows an exploded view of the detector with side muon identifiers.

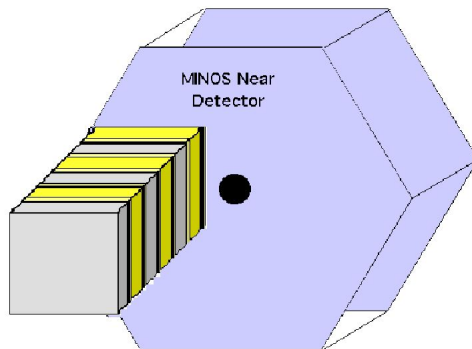


Figure 14: A cartoon view showing the solid scintillator detector in relation to the (much compressed) MINOS near detector

Figure 16 is an example of the granularity of the detector. The event is a charged current ν interaction with $E_\nu = 11.5$ GeV, $x_{Bj} = 0.34$ and $y = 0.94$. Both the x and y stereo views are shown.

Readout would be performed with VLPC technology most recently developed at Fermilab for the D0 experiment [70]. As described in this reference, VLPCs are solid state

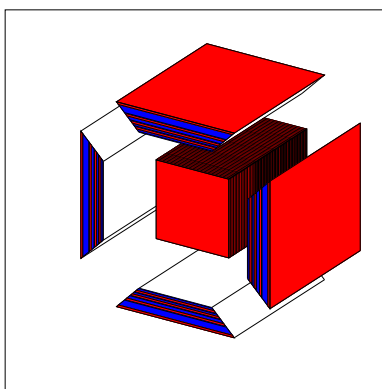


Figure 15: The central detector surrounded by the side muon identifiers consisting of layers of scintillator and (permanent magnet?) steel

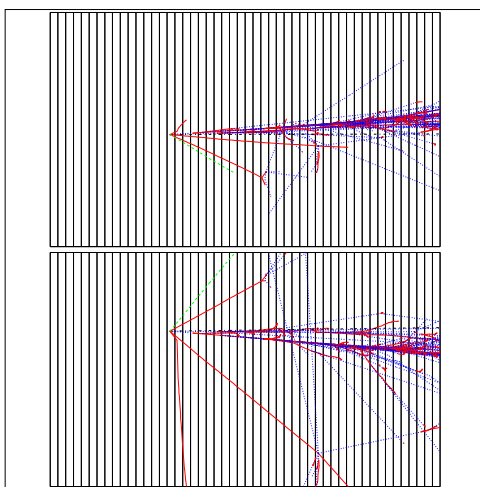


Figure 16: An 11.5 GeV charged current ν interaction in the fine-grained central detector

photodetectors invented at Rockwell International and presently being developed and manufactured by Boeing. They have extremely high quantum efficiency ($\approx 80\%$), high gain, and low gain dispersion. To achieve these impressive characteristics they must be cooled to a few degrees Kelvin. Recent developments since the completion of the D0 installation [71] have indicated that the necessary pixel size for the readout can be appreciably decreased without significantly lowering the quantum efficiency thus decreasing the total cost.

This is not the only detector technique that would meet our goals however, as of now, it appears to be the least expensive detector technology which would meet the goals and, with the establishment of the Fermilab Scintillator/VLPC R&D Facility, a very well-supported technique at Fermilab.

With such a detector, for the initial energy-dependent MINOS run given earlier, two such cycles (32 months running) would result in **2.6 M events** in the fiducial volume of

the scintillator while for a 1 year he-configuration ν run, the corresponding statistics would be **4.9 M events**.

4.1.1 Particle Identification

The identification of the muon for charged current events will be accomplished by minimal passage through the iron/steel of either the MINOS near detector or the side muon identifiers.

Besides observing the low-energy secondaries decaying or stopping, the most powerful means of particle identification, particularly for the relatively low secondary momenta of this experiment, will be Time-of-Flight (TOF). Figure 17 indicates the resolving power of a 2 meter TOF system. The (red) circles show the K^0 -neutron separation and the (green) squares the π -K separation.

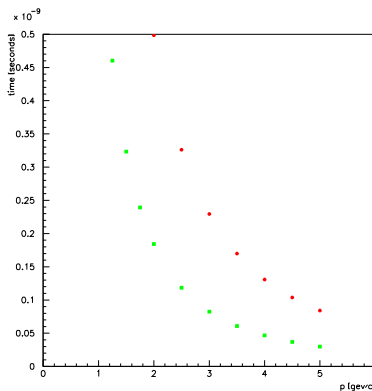


Figure 17: The flight time separation over a 2m path-length for K^0 -n (dark circles) and π -K (light squares) of a given momentum

Particle identification through time-of-flight has another advantage in that there may be an existing TOF system from another experiment which we would be able to adapt to our needs at minimal cost. If this is not possible then using technology developed for this purpose by CDF (Winston cones) or the resistive-plate technology developed by Atlas should be possible at reasonable costs.

Should it prove necessary, another powerful method of particle identification at these low-energies is dE/dx . Figure 18 shows dE/dx for different particle masses as a function of momentum.

4.2 LH_2 and LD_2 Targets

In a subsequent stage it would also be most beneficial, for all physics topics of interest, to have a LH_2/LD_2 target. An investigation of the technical and safety challenges of such a target is currently underway at Fermilab and a recent update indicates that there are

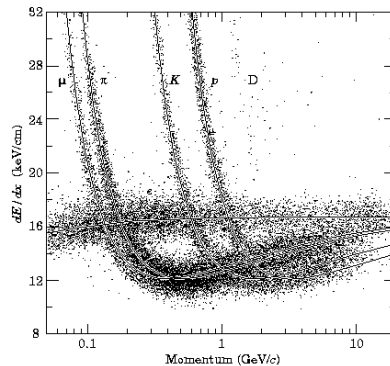


Figure 18: The expected dE/dx for muon, pions, kaons and protons in gas.

no real technical challenges in fabricating or efficiently operating a large LH_2/LD_2 target. The main effort (and expense) for such a facility would be in satisfying safety requirements. For a fiducial volume with $r = 80$ cm. and $l = 150$ cm. we would expect 350 K CC events in LH_2 and 800 K CC events in LD_2 per year of $he-\nu$ running.

5 An Initial Look at Representative Physics Results with the Detector

5.1 Measuring Δs

For the measurement of Δs , a GEANT model indicates that this detector is reasonably hermetic up to a proton energy of several hundred MeV, giving a reasonable Q^2 range for elastic neutrino scattering. The model also indicates that the detector behaves like a sampling calorimeter for low energy hadrons and the resolution is currently being studied.

As an example of the potential of such a detector at the NuMI beam for this measurement, the sensitivity to Δs can be seen in Figure 19. The ratio of the neutral current to charge current yields is shown as a function of Q^2 for three different values of Δs (0.1, 0.0 and -0.1). A measurement of this ratio to an accuracy of 3% would give a determination of Δs to 0.02.

The sensitivity of the ratio of the neutral current to charge current yield to the axial dipole mass is illustrated in Figure 20. Here, the ratio was estimated for the same assumptions as those for Figure 19, however, G_s was held at zero while the axial mass, M_A varied between 1.0 and 1.1, the full range of the uncertainty. The statistics in the figure correspond to a 1 year $he-\nu$ run, which is equivalent to 40 % more elastic events than the MINOS 3-year-run. The trend, the smaller the Q^2 the less dependence on M_A , is independent of statistics.

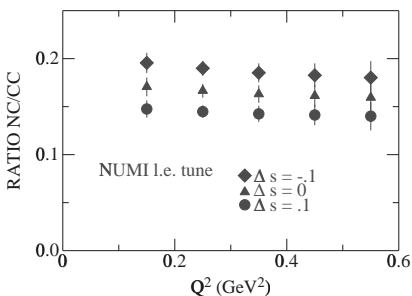


Figure 19: The ratio of the neutral current yield to charge current yield as a function of Q^2 for various values of Δs . The errors correspond, roughly, to the MINOS 3-year-run statistics

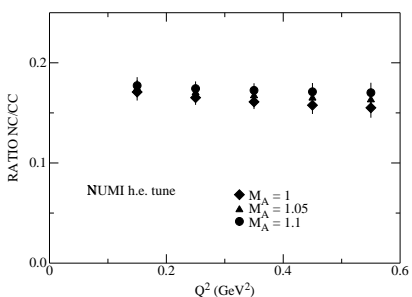


Figure 20: The ratio of the neutral current yield to charge current yield as a function of Q^2 . See text regarding statistics. The yield was estimated for three values of the axial dipole mass ranging from 1.0 GeV to 1.10 GeV.

5.2 Measuring Nuclear Effects

For the study of nuclear effects a selection of nuclear targets would be installed within the scintillator based detector. As an example, 1 ton of C, Fe and Pb were included in the simulation as eleven planes of pure C, three planes of Fe and 2 planes of Pb. The following table summarizes the event rates during the initial MINOS run and a subsequent he ν run for the scintillator plus nuclear target detector concept described here:

CC Event Rates		
Target	MINOS 2-cycle	1 year he ν
CH	2.6 M	4.9 M
C	860 K	1575 K
Fe	860 K	1575 K
Pb	860 K	1575 K

Just over 20% of the above event rates have $x_{Bj} \leq 0.10$. The (approximate) statistical accuracy for measurements of the nuclear effects in the ratios of Fe to C events at small x (shadowing region) are summarized in the following table. The columns designated DIS implies that a cut has been made to keep only events with $W \geq 2.0$ and $Q^2 \geq 1.0$. For the MINOS DIS analysis, the first three bins could be combined into two bins to reduce the statistical errors.

Ratio Fe/C: \sim Statistical Errors				
x_{Bj}	MINOS 2-cycle	MINOS DIS	he ν 1 year	he ν DIS
0.0 - .01	1.8 %	xxx	1.3 %	xxx
.01 - .02	1.4	10 %	1.0	9 %
.02 - .03	1.3	6	1.0	5
.03 - .04	1.2	4	≤ 1	3.2
.04 - .05	1.1	3	≤ 1	2.1
.05 - .06	1.1	2.6	≤ 1	1.7
.06 - .07	1.0	2.3	≤ 1	1.4

Assuming the magnitude of shadowing as predicted by Kulagin, the measured ratio of Fe/C, with statistical errors corresponding to the data accumulated during the MINOS run, would be as in Figure 21. The ratios plotted are for all events. The statistical errors would increase as indicated in the above table when making a DIS cut.

The statistics from the first 3-year MINOS run would be adequate to perform many of the physics topics listed in this paper although some would be limited by the kinematic reach of the neutrino beam energies used for MINOS running. In addition, all studies involving $\bar{\nu}$ statistics would be impossible with only the approved MINOS (ν) exposure. To realize the **full potential** of the NuMI facility for a ν scattering experiment, the impressive statistics and kinematic reach of he-beam 1-year ν and 2-year $\bar{\nu}$ runs would be required.

Ratios(he- ν , 1 year, DIS): \sim Stat. Errors		
x_{Bj}	Fe/C	Fe/LD ₂
.01 - .02	9 %	11 %
.02 - .03	5	6
.03 - .04	3	4
.04 - .05	2	3
.05 - .06	1.7	2
.06 - .07	1.4	1.7

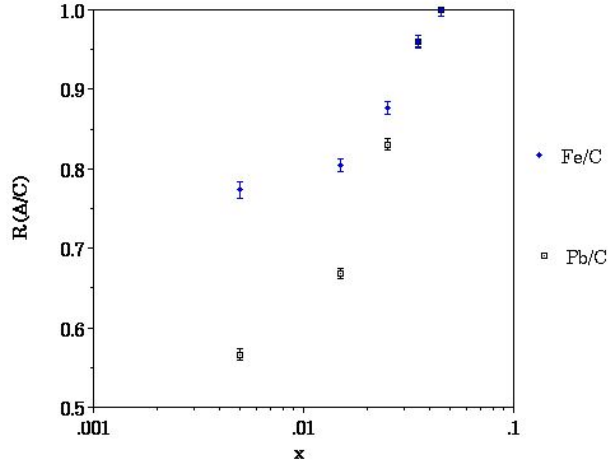


Figure 21: Kulagin’s predicted ratio of shadowing effects off Fe and C targets with the expected errors from all events from the MINOS run.

This large sample of events would allow extraction of the nuclear effects on the individual structure functions F_2 and $x F_3$ via the ratios of Pb and Fe to D_2

5.3 Studying the High- x_{Bj} Region

Using the scintillator, LH_2 and LD_2 samples for the study of the high- x_{Bj} region would yield the following statistical errors on sample size with DIS cuts:

High x_{Bj} (he- ν , 1 year, DIS): \sim Stat. Errors				
x_{Bj}	CH	LH_2	LD_2	
.60 - .65	0.6 %	2.2 %	1.5 %	
.65 - .70	0.7	2.6	1.7	
.70 - .75	1.0	3.7	2.5	
.75 - .80	1.3	5	3	
.80 - .85	2	7	5	
.85 - .90	3	11	7	
.90 - .95	5	17	12	
.95 - 1.0	7	25	17	

The allowable size of the x-bins at high- x_{Bj} will depend on the accuracy with which the hadron energy can be measured. This is currently under study.

5.4 Λ^0 Production in an $\bar{\nu}$ Run

As an example of the statistics expected for strange particle production, the number of Λ^0 's expected via the reaction $\bar{\nu}_\mu + p \rightarrow \mu^+ + \Lambda^0$ in the 2-year he-configuration $\bar{\nu}$ run are shown in the following table:

Total $\bar{\nu}$ events and Λ^0 yield		
target	$\bar{\nu}$ interactions	Λ^0 yield
CH	2700 K	432 K
C-Fe-Pb	900 K each	145 K each
H ₂	200 K	35 K
D ₂	460 K	90 K

As well as significantly increasing the sample of observed and studied strange particle production by $\bar{\nu}$, this experiment could significantly extend the limit on or, perhaps, discover evidence for the existence of SCNC.

6 Conclusions

This collaboration of Nuclear Physics and Elementary Particle Physics groups has suggested that a comparatively small, active detector placed in the NuMI beam at Fermilab can address a wide variety of outstanding neutrino scattering physics issues. Among the topics to be studied would be low-energy neutrino cross-sections and the nuclear effects on observed final states and ν energy distributions, which are of importance to neutrino oscillation experiments.

An initial conceptual design of the proposed detector has indicated that the requirements can be met with existing technology. This proposed technology is currently being further refined at a Fermilab facility dedicated to this purpose.

With an encouraging response to this EOI, we will continue more detailed studies of the physics issues, expand the collaboration within both the EPP and NP communities and proceed with optimization of the detector.

References

- [1] D. Casper *et al.* eds., 'Physics Potential and Feasibility of UNO', June 2001.
- [2] D. Ayres *et al.*, 'Letter of Intent to Build an Off-axis Detector to study $\nu_\mu \rightarrow \nu_e$ oscillations with the NuMI Neutrino Beam', submitted to the Fermilab PAC August, 2002.

- [3] See review article ‘Grand Unified Theories’ and references therein: S. Raby, for the Particle Data Group, Review of Particle Physics (Part I), PRD **66**, 010001-142 (2002).
- [4] Mann, W. A. *et al.*, PRD 34, 2545 (1986).
- [5] M. Apollonio *et al.*, Phys. Lett. B **446**, 415 (1999).
- [6] F. Boehm *et al.*, Phys. Rev. Lett **84**, 3764 (2000).
- [7] C. Mauger, ‘Neutral Current π^0 production in K2K and Super-Kamiokande’, to be published in the proceedings of the NuInt ’01 Conference.
- [8] Stanley Wojcicki, ‘Background Considerations for the Next Generation $\nu_\mu \rightarrow \nu_e$ Experiment’, NuMI-SIM-884, November 2002.
- [9] P. D. Barnes *et al.*, ”Proposal to Measure Particle Production in the Meson Area Using Main Injector Primary and Secondary Beams” Fermilab Proposal-907, 1998.
- [10] N. V. Mokhov and M. A. Kostin, “Non-Neutrino Particle Flux in the NuMI Near Hall”, contribution to the Workshop on New Initiatives for the NuMI Neutrino Beam, Fermilab, 2002.
- [11] A. Vovenko, ”Total cross sections and structure functions for neutrino interactions in 3-30 GeV energy range and near plans for 1-5 GeV energy range”, submitted to the Proceedings of NuInt01 : The First International Workshop on Neutrino-Nucleus Interactions in the Few GeV Region, (2002).
- [12] Figure 5 through Figure 9 are from M. Sakuda, ”Results from Low-Energy Neutrino-Nucleus Scattering Experiments”, submitted to the Proceedings of 1st Workshop on Neutrino - Nucleus Interactions in the Few GeV Region (NuInt01), Tsukuba, Japan, 13-16 Dec 2001.
- [13] T. Sato, ”Weak Pion Production on the Δ_{33} Resonance Region” Presentation at the 2002 Argonne Nuclear Theory Institute, July 2002.
- [14] This working group is chaired by Joseph Formaggio who can be reached at josephf@phys.columbia.edu.
- [15] D. Rein and L. M. Sehgal, Annals Phys. **133**, 79 (1981).
- [16] E. A. Paschos, L. Pasquali and J. Y. Yu, Nucl. Phys. B **588**, 263 (2000) and contributions to this Workshop. [arXiv:hep-ph/0005255].
- [17] S. Wood, ”Resonance Region to DIS, Quark-Hadron Duality”, submitted to the Proceedings of NuInt01 : The First International Workshop on Neutrino-Nucleus Interactions in the Few GeV Region, (2002).

- [18] E. Bloom and F. Gilman, Phys Rev. Lett. **25**, 1140 (1970)
- [19] I. Niculescu, et al., Phys. Rev. Lett. **85**, 1182 (2000)
- [20] C. Keppel et al., E94110 Collaboration, publication in progress
- [21] A. Airepetian et al., HERMES Collaboration, hep-ex/0209018 (2002)
- [22] T. Forest, et al., Hall B Collaboration, publication in progress
- [23] I. Niculescu, et al. Phys. Rev. Lett. **85**, 1186 (2000)
- [24] M. Arneodo *et al.*, Phys. Lett. **B364** (1995) 107
- [25] A. DeRujula, H. Georgi, and H.D. Politzer, Annals Phys. 103, 315 (1977); Phys. Lett. **B64**, 428 (1977)
- [26] D. Golgov, et al., LHPC and TXL Collaborations, Phys. Rev. **D66**, 034506 (2002)
- [27] A. Bodek and U. K. Yang, arXiv:hep-ex/0203009.
- [28] J.G. Morfin, "Future Deeply Inelastic Scattering Experiments at Fermilab", Nucl.Phys.Proc.Suppl.79:664-670,1999 and P. Reimer, "Nuclear Effects in ν -DIS", contribution to the Workshop on New Initiatives for the NuMI Neutrino Beam, Fermilab, 2002.
- [29] G. P. Zeller *et al.* [NuTeV Collaboration], Phys. Rev. Lett. **88**, 091802 (2002) [arXiv:hep-ex/0110059] and references therein.
- [30] S. Kovalenko, I. Schmidt and J. J. Yang, "Nuclear effects on the extraction of $\sin^2\Theta(W)$," arXiv:hep-ph/0207158.
- [31] A. Pais and S. B. Treiman, Phys. Rev. **178** 2365 (1969).
- [32] N. Cabibbo, "Strange Particle Production by Neutrino and Beta Decay", private communication with N. Solomey, 1999.
- [33] M. Goldberger and S. B. Treiman, Phys. Rev. **111** 354 (1958).
- [34] L. Frankfurt, V. Guzey, M. McDermott and M. Strikman, JHEP **0202**, 027 (2002) [arXiv:hep-ph/0201230].
- [35] S. L. Adler, "Sum Rules Giving Tests Of Local Current Commutation Relations In High-Energy Neutrino Reactions," Phys. Rev. 143, 1144 (1966).
- [36] B.T. Fleming et al., [CCFR Collaboration and NuTeV Collaboration] "A first Measurement of the Low x - Low Q^2 Structure Functions in Neutrino Scattering," Nov 2000. e-Print Archive: hep-ex/0011094.

- [37] A. Bodek and J. L. Ritchie, Nuclear Targets,” Phys. Rev. D **24**, 1400 (1981).
- [38] M. Veltri, ”A study of nuclear effects in neutrino interactions with the NOMAD detector”, submitted to the Proceedings of NuInt01 : The First International Workshop on Neutrino-Nucleus Interactions in the Few GeV Region, (2002).
- [39] O. Benhar, A. Fabrocini, S. Fantoni and I. Sick, Nucl. Phys. A **579**, 493 (1994).
- [40] C.H. Lewellyn-Smith, Physics Reports, **C 3**, 261 (1971).
- [41] S. A. Kulagin, “Nuclear shadowing in neutrino deep inelastic scattering,” hep-ph/9812532.
- [42] K. J. Eskola, V. J. Kolhinen, P. V. Ruuskanen and C. A. Salgado, “Nuclear parton distributions: A DGLAP analysis,” Nucl. Phys. **A661**, 645 (1999) e-Print Archive: hep-ph/9906484.
- [43] S. Kumano, “Determination of parton distribution functions in nuclei,” arXiv:hep-ph/0109152.
- [44] A. C. Benvenuti *et al.* [BCDMS Collaboration], Z. Phys. C **63**, 29 (1994).
- [45] M. Vakili *et al.* [CCFR Collaboration], Phys. Rev. D **61**, 052003 (2000) [arXiv:hep-ex/9905052].
- [46] N. Solomey, “Physics prospects with an intense neutrino experiment,” arXiv:hep-ex/0006021 and “Neutrino Interactions-Strange Particle Production”, contribution to the Workshop on New Initiatives for the NuMI Neutrino Beam, Fermilab, 2002.
- [47] K. Myklebost, Quasielastic Production of Lambda Hyperons in Anti-Neutrino Interactions at the CERN PS, Proceedings, Neutrinos 78 (1978) c37-c41.
- [48] S.J. Barish *et al.*, Phys. Rev. Lett. **33** (1975) 1446.
- [49] This section is a condensed version of the following reference. J. Arrington, R. J. Holt, D. H. Potterveld, P. E. Reimer, J. G. Morfin, C. Horowitz and R. Tayloe, “Neutrino Charged and Neutral Current Elastic Scattering from the Nucleon at NuMI”, (unpublished), ANL, 2001.
- [50] W. M. Alberico *et al.* “Measuring Δs ”, contribution to the Workshop on New Initiatives for the NuMI Neutrino Beam, Fermilab, 2002
- [51] U. K. Yang and A. Bodek, Eur. Phys. J. C **13**, 241 (2000) [arXiv:hep-ex/9908058].
- [52] J. Webb, Thesis ”Measurement of Continuum Dimuon Production in 800-GeV/c Proton-Nucleon Collisions” (New Mexico State Univ., Sept 2002), unpublished.

- [53] J. Pumplin, D. R. Stump, J. Huston, H. L. Lai, P. Nadolsky and W. K. Tung, JHEP **0207**, 012 (2002) [arXiv:hep-ph/0201195].
- [54] R. Hasty *et al*, Science **290**, 2117 (2000); B. A. Mueller *et al*, Phys. Rev. Lett. **78**, 3824 (1997); D. Spayde *et al*, Phys. Rev. Lett. **84**, 1106 (2000).
- [55] K. A. Aniol *et al*, Phys. Rev. Lett. **82**, 1096 (1999); nucl-ex/00060002.
- [56] T. Adams *et al*, hep-ex/9906038.
- [57] W. M. Alberico, S. M. Bilenky, C. Maieron, hep-ph/0102269
- [58] J. Ashman *et al*, Nucl. Phys. **B328**, 1 (1989).
- [59] L. A. Ahrens *et al*, Phys. Rev. D **35**, 785 (1987).
- [60] G. Garvey, Phys. Rev. C **48**, 1919 (1993).
- [61] G. T. Garvey *et al* , Phys. Rev. C **48**, 761 (1993).
- [62] B. Adeva *et al*, Phys. Lett. **B302**, 533 (1993); Phys. Rev. **D 58**, 112002 (1998); B. Adams *et al*, Phys. Lett. **B329**, 399 (1994)
- [63] P.L. Anthony *et al*, Phys. Rev. Lett. **71**, 959 (1993).
- [64] K. Abe *et al*, Phys. Rev. Lett. **74**, 346 (1995); Phys. Rev. Lett. **7 5**, 25 (1995); Phys. Rev. **D 58**, 12003 (1998).
- [65] P. L. Anthony *et al*, Phys. Lett. **B 493**, 19 (2000).
- [66] A. Airapetian *et al*, Phys. Lett. **B 442**, 48 (1998); K. Ackerstaff *et al*, Phys. Lett. **B 404**, 383 (1997)
- [67] U. K. Yang and A. Bodek, Phys. Rev. Lett. **82**, 2467 (1999) [arXiv:hep-ph/9809480].
- [68] K. Varvell *et al*. [BEBC WA59 Collaboration], Z. Phys. C **36**, 1 (1987).
- [69] The original design of this "pure scintillator" detector resulted from a study for "Physics at Fermilab with a New High-Intensity Booster" in May, 2000. J. Arrington, R. Holt, D. Potterveld and P. Reimer from Argonne National laboratory and J.G. Morfin from Fermilab were involved in the original concept of this detector.
- [70] A. Bross, E. Flattum, D. Lincoln, S. Grunendahl, J. Warchol, M. Wayne and P. Padley, "Characterization And Performance Of Visible Light Photon Counters (Vlpcs) For The Upgraded D0 Detector At The Fermilab Tevatron," Nucl. Instrum. Meth. A **477** (2002) 172.
- [71] A. Bross, Private Communication

- [72] H. L. Lai *et al.*, Phys. Rev. D **51**, 4763 (1995) [arXiv:hep-ph/9410404].
- [73] H. Deden and et al., [Gargamelle Neutrino Collaboration], “Experimental Study Of Structure Functions And Sum Rules In Charge Changing Interactions Of Neutrinos And Anti-Neutrinos On Nucleons,” Nucl. Phys. **B85**, 269 (1975).
- [74] J. Kilmer and T. J.Sarlina, “Technical and Safety Considerations of Large Cryogenic Liquid Targets at the NuMI Near Hall” contribution to the Workshop on New Initiatives for the NuMI Neutrino Beam, Fermilab, 2002